JOC The Journal of Organic Chemistry

Article

pubs.acs.org/joc

Enhanced Reactivity in Dioxirane C−H Oxidations via Strain Release: A Computational and Experimental Study

Lufeng Zou,[†] Robert S. Paton,*[,†,‡] Albert Eschenmoser,[§] Timothy R. Newhouse,[∥] Phil S. Baran,[∥] and K. N. Houk*[,†]

[†]Department of Chemistry and Biochemistry, University of California, Los Angeles, California 90095, United States

[‡]Chemistry Research Laboratory, University of Oxford, Mansfield Road, Oxford, OX1 3TA U.K.

[§]Laboratorium für Organische Chemie, ETH Zürich, Wolfgang-Pauli-Strasse 10, CH-8093, Switzerland

[∥]Department of Chemistry, The Scripps Research Institute, La Jolla, California 92037, United States

Supporting Information

ABSTRACT: The site selectivities and stereoselectivities of C−H oxidations of substituted cyclohexanes and *trans*-decalins by dimethyldioxirane (DMDO) were investigated computationally with quantum mechanical density functional theory (DFT). The multiconfiguration CASPT2 method was employed on model systems to establish the preferred mechanism and transition state geometry. The reaction pathway involving a rebound step is established to account for the retention of stereochemistry. The oxidation of sclareolide with dioxirane reagents is reported, including the oxidation by the in situ generated *t*Bu-TFDO, a new dioxirane that better discriminates between C−H bonds on the basis of steric effects. The release of 1,3-diaxial strain in the transition state contributes to the site selectivity and enhanced equatorial C−H bond reactivity for tertiary C−H bonds, a result of the lowering of distortion energy. In addition to this strain release factor, steric and inductive effects contribute to the rates of C−H oxidation by dioxiranes.

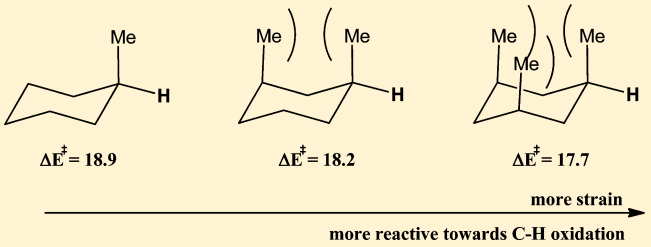

INTRODUCTION

The functionalization of unactivated sp^3 C−H bonds is of considerable interest in contemporary synthetic organic and organometallic chemistry.[1−3] In comparison to traditional functional group manipulations and interconversions employed in synthesis, C−H bond functionalization offers a direct route avoiding prefunctionalization of substrates. However, differentiating between numerous C−H bonds and effecting site-specific and stereoselective chemical modifications is an ongoing challenge.[4] A range of reagents are known for C−H to C−OH conversion, such as Fe-, Cu-, Ru-, Cr-, and Pd-based systems.[5] The pioneering work of Murray[6] and Curci[7] pointed to the use of dimethyldioxirane (DMDO) and methyl(trifluoromethyl)dioxirane (TFDO) for sp^3 C−H oxidation.[8] The dioxiranes are potent oxidants that lead to conservation of stereochemistry, but no intermediate was characterized.[9] The mechanism is still under an ongoing debate, and radical products are observed in some experiments.[10−12] Due to their high reactivity, dioxiranes are sometimes generated in situ during synthesis.[13]

Recently, a two-phase strategy for terpene total synthesis was invented to holistically mimic the way such molecules are constructed in nature. In the first phase, the so-called "cyclase phase", simple terpenes at low oxidation states are stitched together as a prelude to the "oxidase phase", wherein these molecules are systematically oxidized. In the case of the eudesmane terpene class this was done using both innate and guided C−H functionalization logic.[4] The purpose of this strategy for retrosynthetic analysis is not to necessarily recapitulate biosynthesis but rather to uncover new basic reactivity principles and invent new reaction methodology.

The factors that contribute to site selectivity in C−H oxidation reactions has been a question of interest for some time and continues today.[14] Terpenoids contain a host of cyclohexane derivatives, and the rationalization of reactivities in such systems traces back to Barton's fundamental work in the 1950s.[15,16] Reactivity differences, such as those observed for the oxidation of axial and equatorial secondary alcohols with chromic acid, were explained by steric effects. Eschenmoser interpreted the enhanced oxidation rates of axial alcohols in comparison to their equatorial epimers as resulting from the release of 1,3-diaxial strain in the transition state of the oxidation of the axial epimers.[17] Experimental measurements of the rates and regioselectivites of C−H oxidation of substituted cyclohexanes by dioxiranes were performed by Curci,[18,19] and a preference for equatorial attack was observed. Furthermore, Curci[8] and others[20] delineated a variety of factors that contribute to site selectivity in oxidations by dioxiranes. Similar factors have also been reported by White in C−H oxidation

Received: February 20, 2013
Published: March 5, 2013

   dx.doi.org/10.1021/jo400350v | J. Org. Chem. 2013, 78, 4037−4048

reactions of complex molecules by a non-heme, iron-based system.[21,22] This field has a storied history and has been extensively reviewed recently.[23]

In the context of Eschenmoser's hypothesis based on strain release, a recent example of site-selective C−H oxidation of a substituted decalin from Baran's laboratory has been rationalized.[24] Of five unactivated tertiary C−H bonds in the substrate, only equatorial C−H^1 is oxidized to an alcohol by the dioxirane reagent (Scheme 1). Strain release in the transition state was

Scheme 1. Selective C−H Oxidation[a]

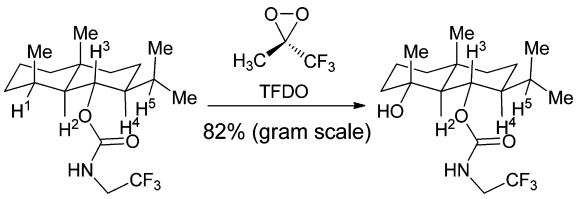

[a]Only one of the five tertiary C−H bonds is oxidized.[24]

proposed to account for the preference.[25] On the basis of computational studies from the Houk[26] and Bach[27] laboratories, a flattening at the carbon undergoing oxidation is expected in the transition structure, which alleviates the 1,3-diaxial strain between two axial methyl groups in the transition state for H^1 abstraction and lowers the activation energy for C−H^1 oxidation.

Given the intensive efforts underway to develop substrate-controlled selective C−H activation processes, we undertook calculations at the density functional and multiconfigurational ab initio levels of theory to gain quantitative insights into the exquisite selectivities reported by Baran. Here we describe computational studies of the transition structures for C−H oxidation of Baran's eudesmane decalins and a variety of other simpler cyclohexanes by dioxirane reagents. We also analyze various substituted cyclohexyl substrates. For several such cases, we report transition structures and present explanations for the enhanced reactivity of equatorial C−H bonds in these strained systems. Additionally, we include a new synthesis of trifluoromethyl *tert*-butyl ketone and its use as a reagent in C−H oxidation by in situ formation of the corresponding dioxirane, *t*Bu-TFDO. A quantitative understanding of the factors contributing to selective C−H activation is provided, in the context of the distortion/interaction theory that has been successfully applied to other types of reactions.[28−31]

COMPUTATIONAL METHODS

All density functional theory (DFT) calculations were performed with Gaussian 09.[32] Mimina and transition structures were optimized using the unrestricted DFT method, UB3LYP, with the 6-31G(d) basis set.[32] Frequency analyses were carried out on stationary points to verify that they are minima or saddle points (transition structures, TSs). Energies were recalculated with UB3LYP/6-311++G(d,p) on these optimized geometries, unless otherwise stated. To ensure that the correct unrestricted wavefunctions were obtained, a stability test was carried out with Gaussian keyword *stable=opt*. Solvation corrections were calculated with the conductor-like polarizable continuum model (CPCM) using the UAHF atomic radii. Multideterminant wavefunction theory, complete active space with second-order perturbation theory (CASPT2) calculations were conducted with MOLCAS 7.4.[33] A 10-electron, 10-orbital active space was employed for CASPT2 calculations with a large cc-pVTZ basis set on the optimized geometries.

RESULTS AND DISCUSSION

Modeling the Dioxirane Oxidation of C−H Bonds. Modeling of dioxirane oxidation has led to different conclusions about the TS geometries. Goddard[34,35] and Bach[36] investigated the electronic structure of dioxirane. The O−O bond lengths in both DMDO and TFDO are 1.51 Å, readily broken due to the ring strain. Early calculations show that a spiro geometry is preferred over a planar geometry for epoxidations.[26,27,37] Houk explored the geometry and selectivities of dioxirane and cyanodioxirane, a model for TFDO, with restricted DFT calculations.[26] Due to the complexity of the potential energy surface (PES), and possible intersystem crossing of the singlet and triplet PES, later studies proposed several different first-order saddle points, associated with three different transition structures[38,39] (Figure 1). We have explored these in more detail in order to determine which is likely to be the most important transition structure for the reaction.

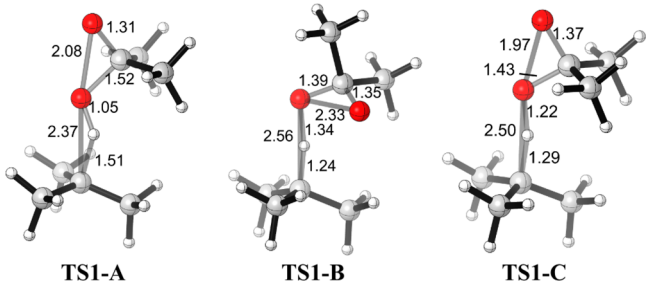

Figure 1. Transition state geometries for the reaction of DMDO and isobutane.

The first transition state, **TS1-A**, is a spiro transition state with all electrons paired, located by restricted DFT calculations.[26,40] This corresponds to a concerted process in which the *tert*-butyl alcohol and acetone are produced without the formation of an intermediate. A wavefunction stability test, however, reveals that this wavefunction is unstable with respect to an unrestricted wavefunction. That is, an open-shell wavefunction is lower in energy. The closed-shell treatment was further invalidated with the multideterminant CASPT2, as strong diradical character is observed in the transition state, indicated by the HOMO/LUMO occupation number of 1.52/0.49 (Table 1).

Table 1. Natural Orbital Occupancies of Frontier Orbitals and Activation Energies in the Transition States[a]

	HOMO	LUMO	CASPT2	UB3LYP[b]
TS1-A	1.42	0.58	21.5	19.9[c]
TS1-B	1.24	0.76	22.5	15.8
TS1-C	1.64	0.37	19.5	20.0

[a]CASPT2(10,10)/cc-pVTZ. Energies are given in kcal/mol. [b]UB3LYP/6-311++G(d,p). [c]24.2 kcal/mol with RB3LYP/6-311++G(d,p).

The second TS, **TS1-B**, has the O−O bond perpendicular to the breaking C−H bond. This is found to be a radical hydrogen abstraction process beginning from the 1,3-dioxy radical. The resulting radical intermediates could then recombine to transfer the OH group to form the products. For this mechanism, the rate-limiting step is the dissociation of the DMDO O−O bond from the singlet diradical, which requires an activation enthalpy

dx.doi.org/10.1021/jo400350v | J. Org. Chem. 2013, 78, 4037−4048

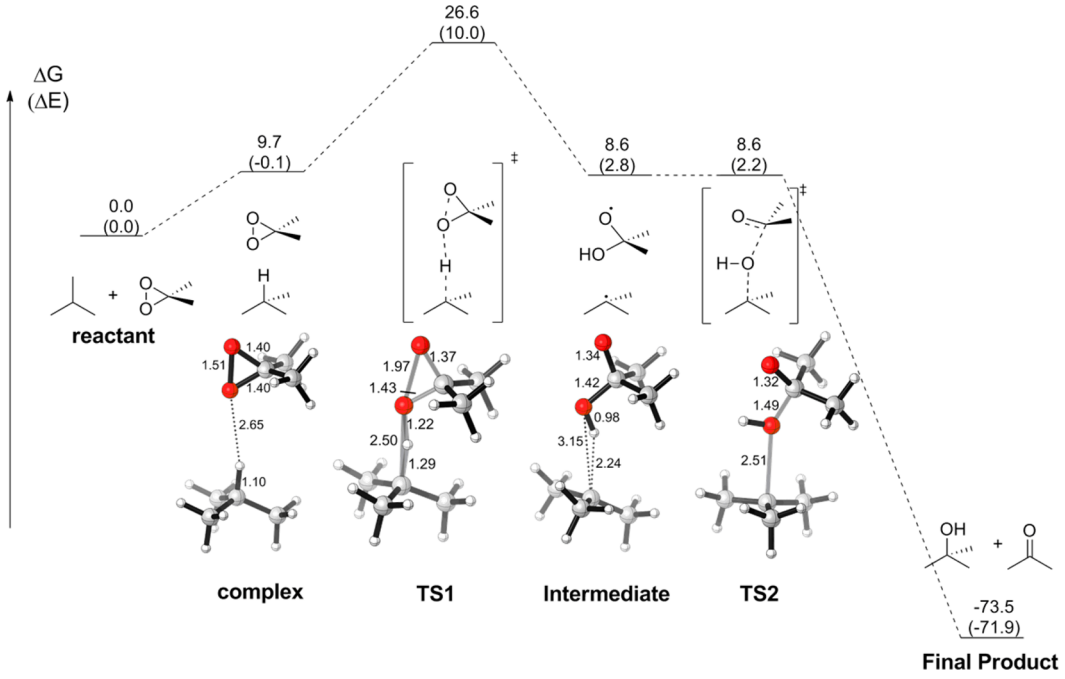

Figure 2. Reaction pathway in DMDO oxidations. Energies are given in kcal/mol.

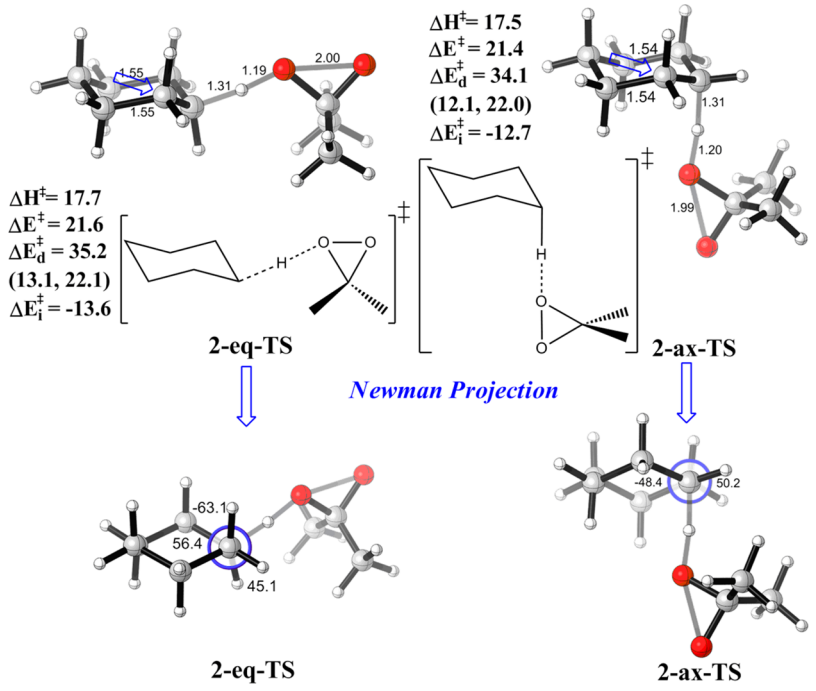

Figure 3. Optimized TSs for the reactions of DMDO with equatorial (**2-eq-TS**) and axial (**2-ax-TS**) C−H bonds. Energies are given in kcal/mol with respect to the corresponding reactants. Individual components of distortion energies (alkane distortion, dioxirane distortion) are given in parentheses.

of 23.1 kcal/mol according to Cremer.[41] The bond-dissociation rate-determining step has a higher barrier than all three C−H activation barriers in Table 1; thus, it is disfavored under kinetic control.

The third TS, **TS1-C**, has the O−O bond aligned with the breaking C−H bond. We use *stable=opt* to obtain the correct wavefunction at the initial geometry and then perform each geometry optimization for the transition state using the optimized wavefunction as an initial guess with the Gaussian keyword *guess=read*. To make sure the optimized geometries have the correct wavefunction, the same procedure was repeated on the optimized geometries. Both the UB3LYP and CASPT2 indicated slight diradical character for the transition state, with $\langle S^2 \rangle$ = 0.5312 with B3LYP and the HOMO/LUMO occupation numbers 1.64/0.37 with CASPT2. Therefore, **TS1-C** is the most reliable transition state. As CASPT2 becomes formidably expensive with larger systems, UB3LYP with the stable open-shell wavefunction was employed for further studies.

dx.doi.org/10.1021/jo400350v | J. Org. Chem. 2013, 78, 4037−4048

Table 2. Summary of Activation Energies and Distortion/Interaction Energies (kcal/mol)

Compound	C-H bond for oxidation	$\Delta H^{\ddagger}$	$\Delta E^{\ddagger}$	$\Delta E_d^{\ddagger}$(alkane)	$\Delta E_d^{\ddagger}$(DMDO)	$\Delta E_d^{\ddagger}$(total)	$\Delta E_i^{\ddagger}$
1	*t*Bu-**H**	16.2	20.0	11.1	21.7	32.7	-12.8
2-eq	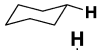	17.7	21.6	13.1	22.1	35.2	-13.6
2-ax		17.5	21.4	12.1	22.0	34.1	-12.7
3-eq	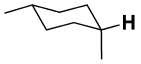	15.4	18.9	10.5	21.6	32.1	-13.2
3-ax	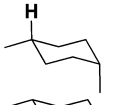	15.8	19.5	10.5	21.6	32.1	-12.6
3'-ax	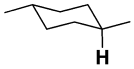	16.1	19.6	10.5	21.6	32.2	-12.6
4-eq	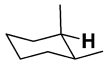	15.3	18.7	10.2	21.5	31.7	-13.0
4-ax	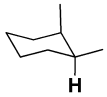	15.8	19.2	10.2	21.5	31.7	-12.5
4'-ax	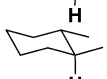	16.4	19.8	10.5	21.7	32.2	-12.4
5-eq	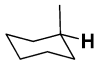	15.4	18.9	10.5	21.6	32.1	-13.2
6	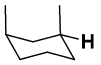	14.7	18.2	9.9	21.3	31.2	-13.0
7	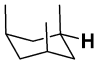	14.2	17.7	9.4	21.1	30.4	-12.8
8[a]	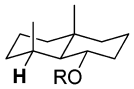	13.3	16.4	10.1	20.2	30.3	-13.9
9[a]	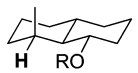	13.5	16.8	10.3	20.6	30.9	-14.1
10-eq-C2	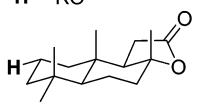	18.3	22.2	12.8	22.1	34.9	-12.7
10-eq-C3	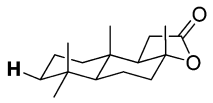	18.8	22.7	13.8	23.8	36.0	-13.3
10-ax-C3		18.5	22.2	12.5	22.1	34.5	-12.3

[a]R = $-C(O)NHCH_2CF_3$. *i*Pr on the decalin ring is omitted.

The mechanism involving **TS1-C** is analogous to the "oxygen rebound" mechanism common in iron−oxo oxidations.[42,43] The complete reaction pathway was then explored and is summarized in Figure 2. The reactant complex goes through C−H activation transition state **TS1** and forms a weakly bound radical pair intermediate, which rebounds and forms the final product. The reaction can be tracked with the forming C−O bond length. As the two reactants approach each other, the C−O bond distance decreases until it reaches a minimum at 2.50 Å in TS1 and then increases back to 3.15 Å after hydrogen abstraction, leaving two radical centers in the intermediate. The C−O bond distance then decreases again ("rebounds") through 2.51 Å in **TS2** to eventually 1.43 Å in the product. As the second transition state has essentially no barrier, the radical pair intermediate is expected to have too short a lifetime to escape from the solvent cage, leading to the retention of stereochemistry as observed in experiments.

The same conclusions hold for the more reactive oxidant TFDO. The C−H activation free energy is around 5 kcal/mol lower with TFDO than with DMDO, but the preferred transition state is again obtained with unrestricted and optimized wavefunctions (Figure S3 for the TS geometry and Table S1 for the natural orbital occupancies in the Supporting Information). The overall reaction pathway is similar and the rate-limiting step is again the C−H activation step with diradical character (Figure S4 in the Supporting Information). On the basis of the similarity of the DMDO and TFDO reaction pathways, the in situ generated *t*Bu-TFDO is expected to follow the same mechanism. The computational results are in agreement with Curci's finding that TFDO is more reactive

dx.doi.org/10.1021/jo400350v | J. Org. Chem. 2013, 78, 4037−4048

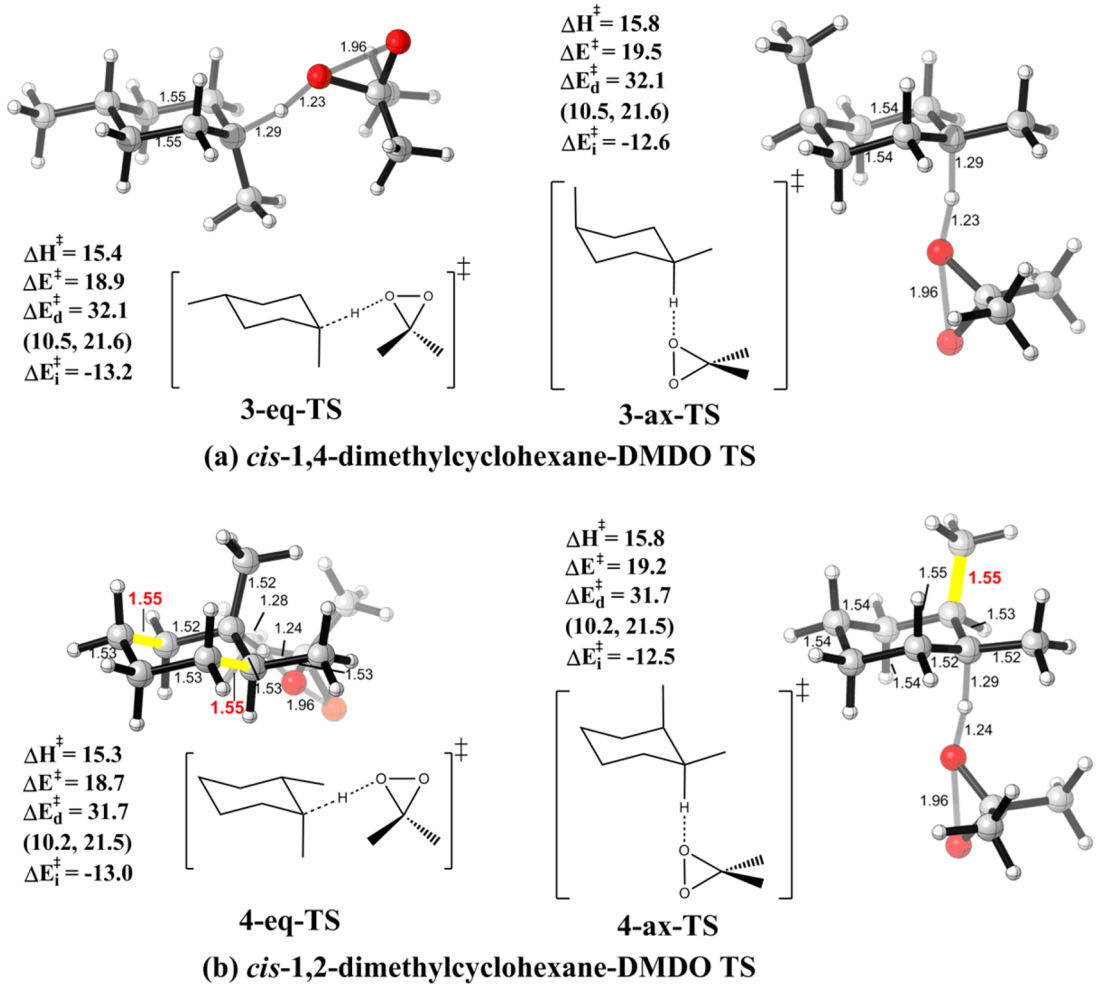

Figure 4. Optimized TSs for the reactions of DMDO with (a) *cis*-1,4-dimethylcyclohexanes at the equatorial (**3-eq-TS**) and axial C−H bonds (**3-ax-TS**) and (b) *cis*-1,2-dimethylcyclohexanes at the equatorial (**4-eq-TS**) and axial (**4-ax-TS**) C−H bonds. Energies are given in kcal/mol with respect to the corresponding reactants. Individual components of distortion energies (alkane distortion, dioxirane distortion) are given in parentheses.

than DMDO without diminished selectivity, as an exception to the reactivity−selectivity rule.[9]

Oxidation of Equatorial and Axial C−H Bonds of Cyclohexane. The TSs for axial and equatorial C−H oxidation by DMDO are shown in Figure 3. No significant axial/equatorial preference is found. The activation energy for oxidizing the cyclohexane equatorial hydrogen is 21.6 kcal/mol, while for the axial hydrogen it is 21.4 kcal/mol.

To evaluate the factors governing relative reactivities of C−H bonds quantitatively, a distortion/interaction energy analysis was conducted. The distortion energy ($\Delta E_d^{\ddagger}$) is the energy required to distort the reactants, hydrocarbon plus the oxidant dimethyldioxirane (DMDO), into the transition state (activated) geometry. The interaction energy ($\Delta E_i^{\ddagger}$) is the energy lowering due to the interaction of the two distorted reactants. Distortion energies favor attack on the axial hydrogen by 1.1 kcal/mol, while interaction energies favor equatorial attack by 0.9 kcal/mol. These two components largely cancel out, leaving essentially no preference (0.2 kcal/mol). The nearly identical activation energies for **2-eq-TS** and **2-ax-TS** indicate very weak axial/equatorial selectivity, if any, as observed experimentally for C−H activations of different types.[25]

The distortion of the DMDO moiety is about the same for both transition states, and the difference in the distortion energies mainly comes from the cyclohexane distortion. Hyperconjugation is a likely factor in the 0.9 kcal/mol difference in interaction energies (Figure 3). In **2-eq-TS**, there are two C−C bonds *anti* to the breaking C−H bond, while there are two antiperiplanar C−H bonds in **2-ax-TS**. The hyperconjugative stabilization of the partial positive charge in the polarized transition states is larger in **2-eq-TS**.[20] A slight lengthening of the antiperiplanar bonds is observed in the optimized transition structures, indicative of this hyperconjugative interaction.

The distortion energy difference can be attributed to torsional interactions. The Newman projections of these two transition states are given in Figure 3. The internal C−C−C−C dihedral angle is 56° in **2-eq-TS**, slightly more distorted than that in cyclohexane (55°). This angle is 48° in **2-ax-TS**, closer to the more relaxed angle in the cyclohexyl radical (44°). The relaxation is reflected as a 1.0 kcal/mol lowering in the distortion energy. Hydrogen−hydrogen repulsion also plays a part in the relative stability. As hydrogen is being abstracted from a tetrahedral sp^3 carbon, the carbon flattens and becomes sp^2 in character. As shown in the Newman projection for **2-eq-TS**, this leads to slightly greater eclipsing of the vicinal C−H bonds, as indicated in the 45° dihedral angle, while that in **2-ax-TS** is 50°. Therefore, the distortion energy for **2-eq-TS** is higher. This torsional effect favoring axial attack was observed in the case of nucleophilic attack on cyclohexanone (Felkin's

dx.doi.org/10.1021/jo400350v | J. Org. Chem. 2013, 78, 4037−4048

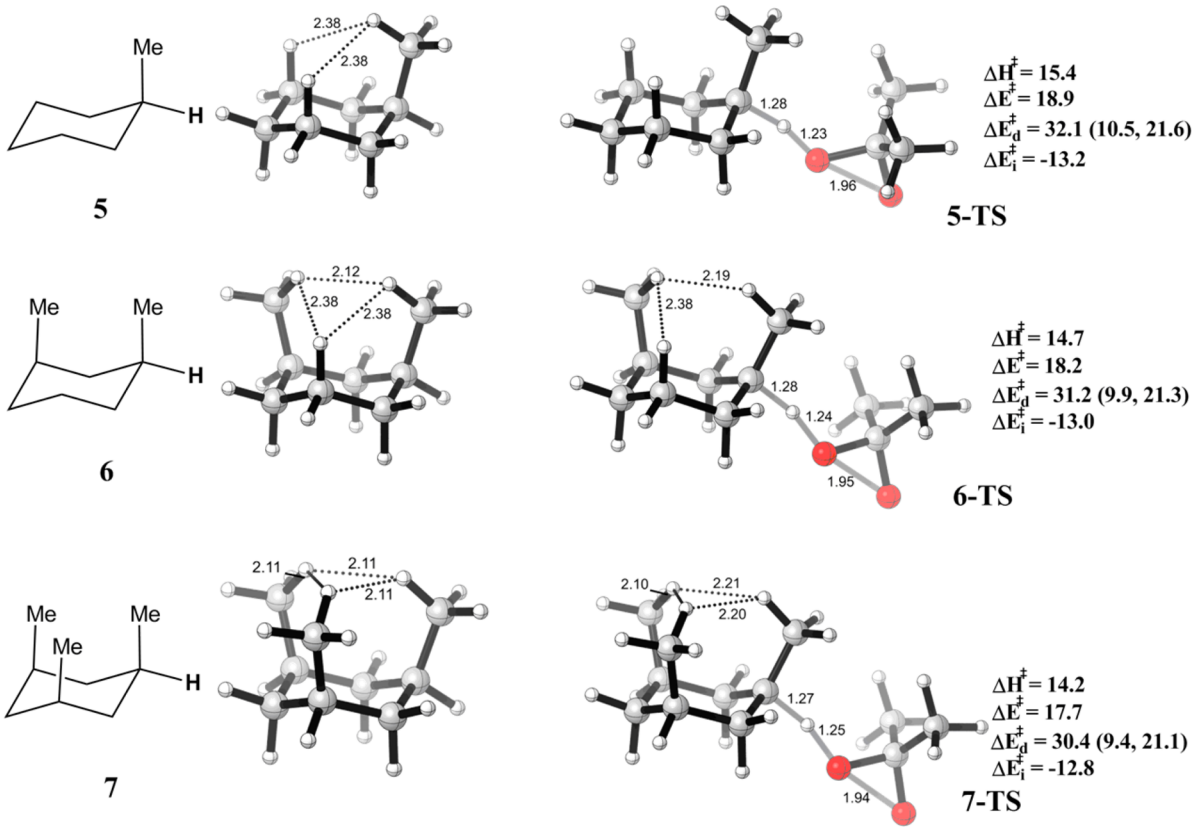

Figure 5. Optimized reactant and transition state geometries for the reaction of DMDO with substituted cyclohexanes. Energies are given in kcal/mol. Individual components of distortion energies (alkane distortion, dioxirane distortion) are given in parentheses.

rule)[44,45] and reactions of cyclohexyl radicals,[46] in which the axial TS has a more staggered conformation than the equatorial TS. In the reactions studied here, the cancellation of distortion and interaction energy preferences leads to no intrinsic selectivity for the secondary C−H bonds of cyclohexane.

This type of analysis has been performed on a variety of cyclohexanes and decalins. The results are tabulated in Table 2.

Oxidation of Methylcyclohexane. The TSs for tertiary axial/equatorial C−H oxidation of *cis*-1,4-dimethylcyclohexane by DMDO are shown in Figure 4a, as a eudesmane model system with both axial and equatorial tertiary C−H bonds. The activation energy for the reaction of the equatorial C−H bond in **3-eq-TS** is 0.6 kcal/mol lower than that for the axial C−H bond in **3-ax-TS**. While interaction energies again favor equatorial hydrogen abstraction, the distortion energies are essentially the same. The axial/equatorial selectivity comes from the interaction energies, which are −13.2 kcal/mol for **3-eq-TS** and −12.6 kcal/mol for **3-ax-TS**. This preference, coming from interaction energies, is found again in **4-eq-TS** and **4-ax-TS**, where both axial and equatorial C−H bonds are present in the same molecule (Figure 4b).

The distortion energies are identical for the two transition states, while the interaction energies are −13.0 and −12.5 kcal/mol, respectively. Just as in the case of secondary hydrocarbons, the lengthening of antiperiplanar C−C bonds is shown in the equatorial TS, leading to better hyperconjugation. A more detailed study of how distortion energies change along the reaction coordinate is summarized in Figure S1 in the Supporting Information. Distortion energies are the same, since the tertiary C−H oxidation transition states are earlier than the transition states for secondary C−H oxidation. With the same distortion energy and favored interaction energy for abstraction of equatorial hydrogens, the latter is slightly more susceptible to oxidation.

The stereochemistry of the remote methyl group has no effect on the reactivity; only the stereochemistry of the carbon on which hydrogen is abstracted matters. As in Table 2, axial C−H oxidations give almost identical distortion and interaction energies for *cis*-1,4-dimethylcyclohexane (**3-ax**) and *trans*-1,4-dimethylcyclohexane (**3′-ax**), leading to the same activation energy.

The stereochemistry of the methyl group α to the reacting center has little impact on the interaction energy, which is intrinsic whether an axial or equatorial hydrogen is abstracted. As in Table 2, oxidation of *cis*-1,2-dimethylcyclohexane (**4-ax**) and *trans*-1,2-dimethylcyclohexane (**4′-ax**) give virtually identical interaction energies. The distortion energy for **4′-ax** is raised by 0.5 kcal/mol due to developing torsional strain in the transition state as the reacting site becomes more sp^2 in character. Overall the activation energy for **4′-ax** is 0.6 kcal/mol higher than that of **4-ax**.

In comparison with tertiary C−H bonds, activations of secondary C−H bonds require higher activation energies, which are around 21.5 kcal/mol in Figure 3 due to the electrophilic nature of the oxidizing reagent, compared with those activation energies for tertiary C−H bonds, which are below 20.0 kcal/mol. This agrees with Curci's experiments that tertiary C−H bonds are generally more reactive than secondary C−H bonds and the usual greater stability of tertiary radicals.[17] The differences in activation energies between secondary C−H oxidation (∼18 kcal/mol) and tertiary C−H oxidation (15−16 kcal/mol) is comparable to, or slightly higher than, the

dx.doi.org/10.1021/jo400350v | J. Org. Chem. 2013, 78, 4037−4048

Scheme 2. Reaction Products in a Competition Reaction

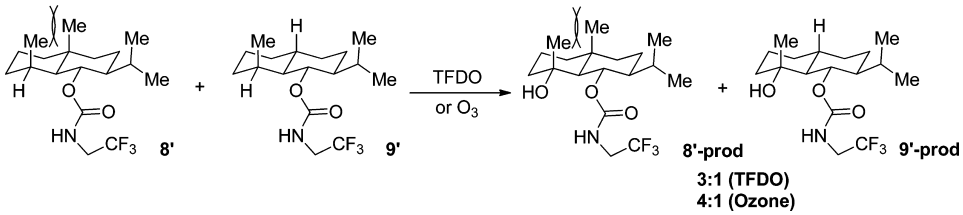

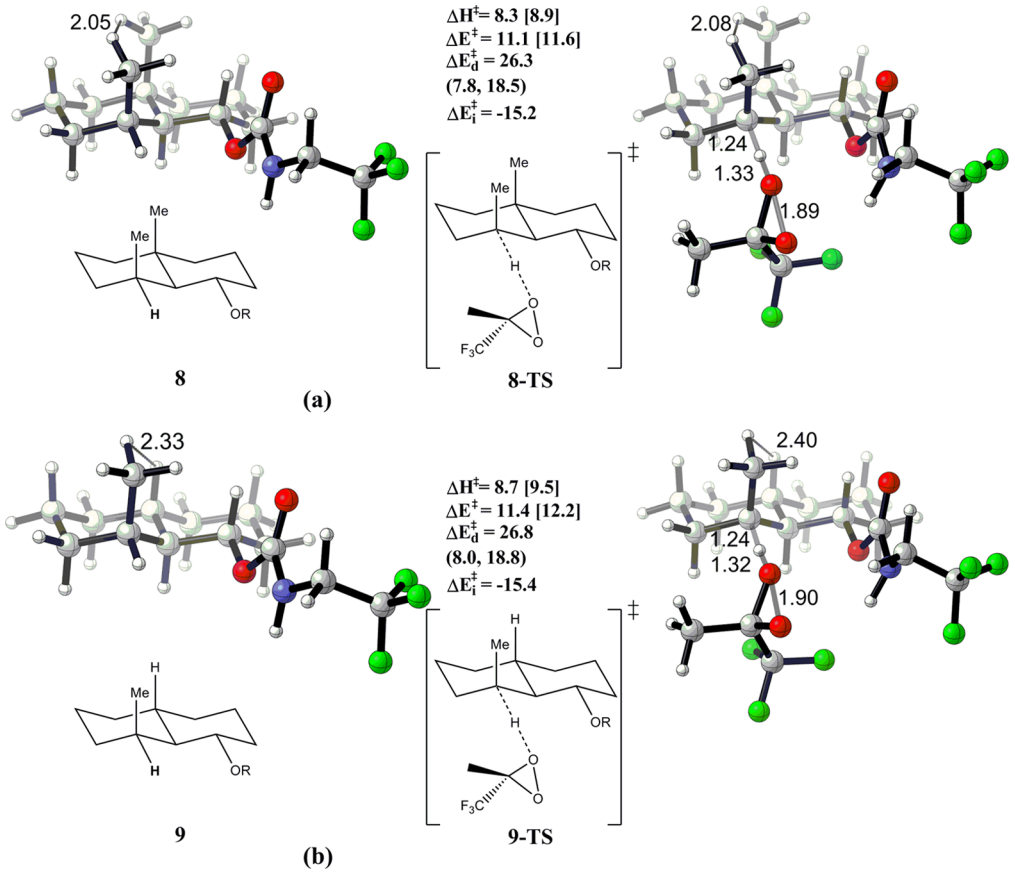

Figure 6. Optimized reactant and transition state geometries for the reaction of TFDO with (a) **8** and (b) **9** (R = $-C(O)NHCH_2CF_3$). The *i*Pr substituents on the decalin rings of **8′** and **9′** are omitted for simplicity. Energies are given in kcal/mol. Individual components of distortion energies (alkane distortion, dioxirane distortion) are given in parentheses. Energies with dichloromethane solvation correction are given in brackets.

difference between secondary and tertiary C−H bond dissociation enthalpies (BDEs) (98 and 96 kcal/mol, respectively[47]) because there is polarization and partial positive charge buildup at the oxidized carbon in the transition states.

Influence of Axial Methyl Substitution on Reactivity. To systematically investigate the effects of 1,3-diaxial methyl−methyl interactions, reactivities of the tertiary equatorial C−H bonds reacting on axial methylcyclohexane (**5**), diaxial 1,3-dimethylcyclohexane (**6**), and triaxial 1,3,5-trimethylcyclohexane (**7**) were studied. The reactants and transition states are shown in Figure 5. The methyl groups in **5**−**7** were axial rather than the more stable equatorial position, to serve as models for rigid terpenes, where the methyl groups are fixed to be axial, as in Baran's selective oxidation of **1**.[24] The relative rate for oxidation of *cis*-1,3-dimethylcyclohexane (**6**) is slightly higher than that for *trans*-1,3-dimethylcyclohexane, as strain release operates in the former isomer, in agreement with a ratio of (1.4−1.5):1 by TFDO oxidation generated in situ.

As more axial methyl substituents were added (**5** to **6** to **7**), the nearest H−H distance gets shorter, and more strain is imposed as the H−H closed shell repulsion increases. In the reactants, there is no significant H−H repulsion in **5**, there is one H−H interaction with a 2.12 Å distance in **6**, and there are three pairs of CH−CH interactions of 2.11 Å in **7**. In the transition state for abstraction of equatorial hydrogens, the methyl bends away from the ring, releasing 1,3-diaxial strain. In **5**, the H−H distances are above 2.4 Å, and no strain is released in the TS. In **6**, the closest H−H bond distance increases from 2.12 Å in the reactant to 2.19 Å in the TS, releasing strain. In **7**, the two closest H−H distances increase from 2.11 to 2.20 and 2.21 Å, and further strain release is expected.

The trend toward lower activation energy was reflected in the decreasing distortion energies, from 32.1 (**5-TS**) to 31.2 (**6-TS**) to 30.4 kcal/mol (**7-TS**). The interaction energies are nearly the same, increasing by 0.2 kcal/mol (less negative) with each additional axial methyl group, but this change is smaller than the increase in distortion energies, which dominates the trend

dx.doi.org/10.1021/jo400350v | J. Org. Chem. 2013, 78, 4037−4048

Table 3. Experimental and Calculated Ratios for C2/C3 Products from 10[a]

oxidant	exptl C2:C3	ref	calcd C2:C3	$\Delta E^{\ddagger}$(C2)	$\Delta E^{\ddagger}(C3_{axial})$	$\Delta E^{\ddagger}(C3_{equatorial})$
DMDO	1.5:1[b]	49	~1:1[c]	22.2[c]	22.2[c]	22.7[c]
TFDO	2.1:1 to 1:2.0[d]	49	2.7:1[e]	10.2[e]	12.1[e]	10.9[e]
*t*Bu-TFDO	2.4:1[f]	49	8.3:1[e]	11.9[e]	14.3[e]	13.1[e]
$Rh_2(esp)_2$[g]	only C2	49				
Mn(TPP)Cl[h]	7:1	50				
Fe(PDP)	1.4:1	21				

[a]Energies are given in kcal/mol. [b]1:1 acetone:DCM, <5% conversion. [c]UB3LYP/6-311++G(d,p), gas phase. [d]Ratios with a variety of solvents gave from 2.1:1 with hexafluoroisopropyl alcohol to 1:2.0 with acetonitrile. [e]UB3LYP/6-311++G(d,p), calculated ratio from activation energies in 298 K with CPCM/UAHF in acetonitrile. [f]In acetonitrile solvent. [g]Amination products. [h]A ratio of 3:1 was observed for fluorination with Mn(TMP)Cl.

Table 4. Analysis of Site Selectivities on 10 for TFDO vs *t*Bu-TFDO[a]

oxidant	TS	$\Delta H^{\ddagger}$(solv)[b]	$\Delta H^{\ddagger}$	$\Delta E^{\ddagger}$	$\Delta E_d^{\ddagger}$(**10**)	$\Delta E_d^{\ddagger}$(TFDO)	$\Delta E_d^{\ddagger}$(**10**+TFDO)	$\Delta E_i^{\ddagger}$
TFDO	**C2**	6.7	12.2	15.7	8.7	20.2	28.9	−13.2
TFDO	**C3-ax**	8.8	12.7	15.9	8.5	20.1	28.6	−12.7
TFDO	**C3-eq**	7.5	12.8	16.1	9.2	20.3	29.5	−13.4
*t*Bu-TFDO	**C2**	8.3	14.2	17.8	9.9	20.8	30.7	−12.9
*t*Bu-TFDO	**C3-ax**	10.7	15.1	18.7	10.3	20.8	31.1	−12.4
*t*Bu-TFDO	**C3-eq**	9.5	15.0	18.7	11.1	20.9	32.1	−13.4

[a]Energies are given in kcal/mol. [b]Calculated solvent with CPCM/UAHF in acetonitrile.

in reactivity. Most of the difference in distortion energy results from the hydrocarbon reactant. The steric acceleration proposed to result from strain release by Eschenmoser[17] is manifested in lower distortion energy in the TS. In other words, the reactants are predistorted toward the TS geometry, and the activation energy is lowered. We have referred to this phenomenon as distortion-acceleration.[48] The higher reactivity along the series is also paralleled by slightly earlier transition states along the series, and so the distortion energy of the dioxirane decreases in the series.

Strain Release and Enhanced Reactivity toward Oxidations in Steroidal Systems. The strain release (or distortion-acceleration) effect has been taken advantage of by Baran[24] to generate selectivity in C−H oxidations, as shown in Scheme 2. A 1:1 mixture of **8′** and **9′** gave the corresponding oxidation products in a ratio of 3:1. The strain release effect was proposed to account for the enhancement in reactivity of **8′** as compared with that of **9′**. A similar trend in reactivity was observed in oxidation by ozone, which produced **8′** and **9′** in a 4:1 ratio.

We modeled the reaction with methyl(trifluoromethyl)-dioxirane (TFDO) and dichloromethane as the solvent. The results are shown in Figure 6. A model study with DMDO and these substrates in the gas phase is summarized in Table 2.

Reactants **8** and **9**, models for **8′** and **9′**, and transition states for DMDO **8-TS** and **9-TS** are shown in Figure 6a and Figure 6b, respectively. In Figure 6a, the two axial methyl groups in **8** lead to strong 1,3-diaxial strain, with the nearest H−H distance being 2.05 Å. This distance becomes 2.08 Å in **8-TS**, which reduces the strain. The remaining H−H distances stay rather constant, contributing little to the activation energies due to strain release. The energy required to distort **8** into **8-TS** is 26.3 kcal/mol, mainly from the dioxirane distortion, due to the stiffness of the ring.

The aforementioned methyl−methyl interaction in **8** is alleviated when the bridge methyl is replaced by a hydrogen atom for **9** in Figure 6b. In comparison with the case for **8**, there is less strain release. In other words, more energy was required to distort the reactant **9** into its transition state **9-TS**, with the distortion energy increased to 26.8 kcal/mol; the activation energy is 11.4 kcal/mol. The 0.5 kcal/mol difference in distortion energy, although rather small, dominates over the interaction energies and leads to 0.3 kcal/mol lower activation energy for **8-TS** than for **9-TS**. With solvent correction, there is a 0.6 kcal/mol decrease in activation enthalpy for **8-TS**, in agreement with the observed 3:1 experimental ratio. For the model study with DMDO, the predicted activation energy for **8-TS** is 0.4 kcal/mol lower than for **9-TS** (16.4 and 16.8 kcal/mol, respectively). The axial methyl group gives only 0.4 kcal/mol rate enhancement for the substituted decalin, in comparison to 0.7 kcal/mol with substituted cyclohexane, which is likely due to the rigidity of the ring, as reflected in the distortion energies of the ring systems.

Selective Oxidations of Sclareolide. Sclareolide (**10**) has 5 methylenes and 10 distinct secondary hydrogens. Experimentally, **10** is oxidized at both the C2 and C3 positions (steroid numbering),[49] and ratios of products are given in Table 3.

Electronically, oxidation of C3 is favored because it is remote from the electron-withdrawing lactone that deactivates the methylenes at C1, C5, and C6 and steric effects favor oxidation at C2. For reagents that behave like small reagents, such as dioxiranes and Fe(PDP), there is marginal selectivity between oxidation at the C2 and C3 positions. The use of a manganese porphyrin results in considerably higher site selectivity.[50] In the case of the Rh-mediated amination employing a reagent that behaves like a large reagent, excellent C3 selectivity is observed.[5n,24]

Table 4 shows details of the computed activation barriers with different oxidants. The bulky *t*Bu group of *t*Bu-TFDO increases the activation energies by about 2 kcal/mol, which is reflected in the distortion energies, especially from the substrate **10**. The interaction energies are essentially the same, since the methyl group in TFDO and *t*Bu in *t*Bu-TFDO have similar electronic effects. The reactants and transition states geometries are shown in Figure 7 for TFDO and Figure 8 for *t*Bu-TFDO. With solvent correction (acetonitrile), the axial TS becomes disfavored, probably due to a higher energy cost for the

dx.doi.org/10.1021/jo400350v | J. Org. Chem. 2013, 78, 4037−4048

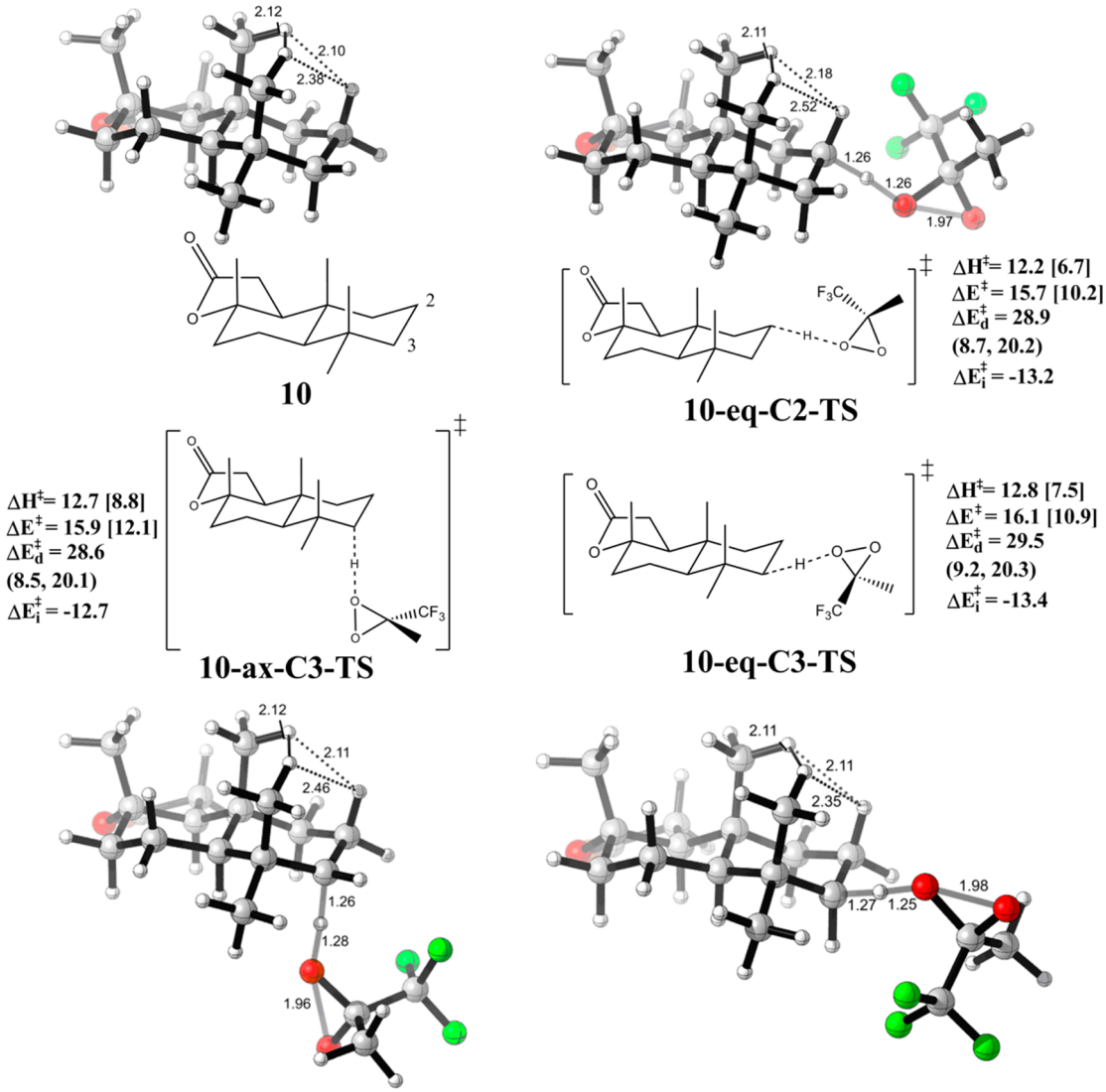

Figure 7. Optimized reactant and transition state geometries for the reaction of TFDO with sclareolide (**10**). Energies are given in kcal/mol. Individual components of distortion energies (alkane distortion, dioxirane distortion) are given in parentheses. Energies with acetonitrile solvation correction are given in brackets.

rearrangement of solvent molecules. Also, a higher C2:C3 selectivity is expected. A thorough study of solvent effects is underway.

Figure 7 gives the geometries of sclareolide (**10**) and three transition states for C−H oxidations on the C2/C3 C−H bonds with TFDO. The methyl hydrogen strain is released, as the bond lengths for nearest H−H pairs, which are 2.10 and 2.12 Å in **10**, increased to 2.11 and 2.18 Å in **10-eq-C2-TS**, but stays the same on **10-ax-C3-TS** and **10-eq-C3-TS**. Not surprisingly, the strain release effect is not as pronounced as is the case with the relief of a methyl−methyl 1,3-diaxial interaction. Accordingly, a mixture of products results.

Figure 8 gives the geometries of sclareolide (**10**) and three transition states for C−H oxidations on the C2/C3 C−H bonds with the bulkier oxidant *t*Bu-TFDO. The site selectivity for oxidation on the C2 versus C3 position is predicted to be 0.9 kcal/mol. Experimentally a higher C2/C3 ratio was observed for *t*Bu-TFDO than for TFDO. The steric effect of the *tert*-butyl group raises the activation barriers for *t*Bu-TFDO oxidations in comparison with TFDO by about 2 kcal/mol. This energy difference is also consistent with the low yield and low levels of reactivity observed with *t*Bu-TFDO in comparison with TFDO. The trace conversion affected by *t*Bu-TFDO may also reflect the low concentration of this reagent in the reaction mixture, as it is formed in situ. The increased steric effects also render the equatorial hydrogen on C3 as susceptible to oxidation as the axial hydrogen at the same position.

■ CONCLUSIONS

The site selectivities and stereoselectivities of sp^3 C−H activations in cyclohexane derivatives by dioxiranes were investigated computationally. CASPT2 calculations established the appropriate transition state for C−H oxidations by dioxiranes, which corresponds to that located using unrestricted DFT. The full pathway for dioxirane oxidation was established. The distortion/interaction model was used to understand the origins of selectivity in each case. In the absence of axial substitution of cyclohexanes there is no innate preference for either axial or equatorial C−H activation: eclipsing interactions slightly favor axial activation, but this is counterbalanced by the greater hyperconjugative stabilization in equatorial activation.

dx.doi.org/10.1021/jo400350v | J. Org. Chem. 2013, 78, 4037−4048

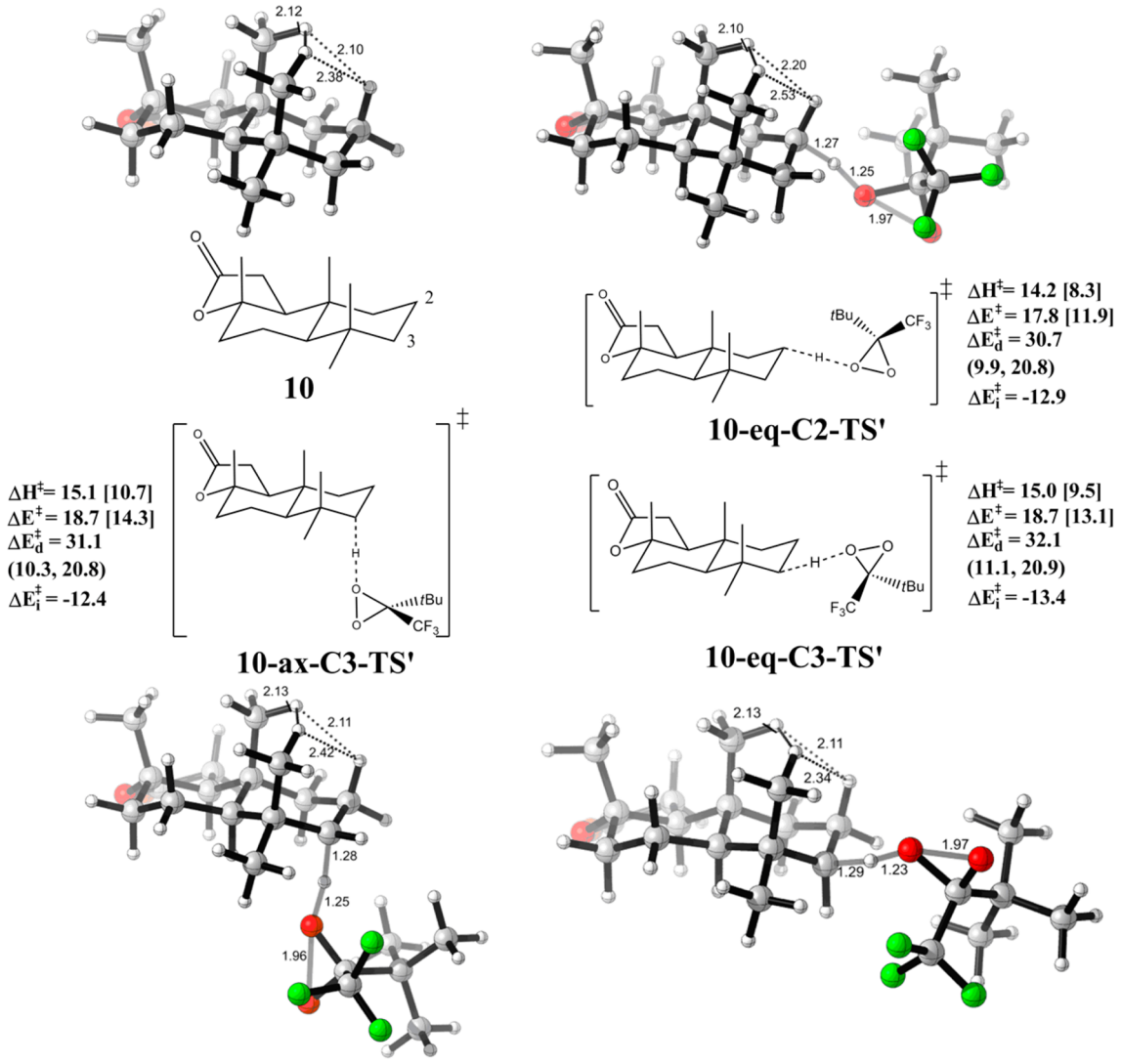

Figure 8. Optimized reactant and transition state geometries for the reaction of *t*Bu-TFDO with sclareolide (**10**). Energies are given in kcal/mol. Individual components of distortion energies (alkane distortion, dioxirane distortion) are given in parentheses. The prime labels on TS distinguish the transition states for *t*Bu-TFDO oxidation from those with DMDO. Energies with acetonitrile solvation correction are given in brackets.

The axial and equatorial C−H bonds of cyclohexane have similar reactivities.

However, with increasing axial substitution, computed activation barriers decrease, in accord with experiment. The enhancement in equatorial reactivity by geminal and diaxial substitution arises as a consequence of strain release in going to the transition state.[25] The distortion/interaction model allows for a quantification of the acceleration that arises as a result of strain release. The strain release effect is around 0.7 kcal/mol when the strain involving two 1,3-diaxial methyl groups is released. The eudesmane **8** is more reactive than **9** due to the strain release effect, but the C2/C3 site selectivity for sclareolide is dominated by steric effects and can be controlled by the bulkiness of the reagents.

EXPERIMENTAL SECTION

General Procedures. All reactions were carried out under an inert nitrogen atmosphere with dry solvents under anhydrous conditions, unless otherwise stated. Dry acetonitrile (MeCN) was obtained by passing the previously degassed solvents through activated alumina columns. Product ratios were determined by analysis of the crude ^{1}H NMR spectra. Yields refer to chromatographically and spectroscopically (^{1}H NMR) homogeneous materials, unless otherwise stated. Reagents were purchased at the highest commercial quality and used without further purification, unless otherwise stated. Reactions were monitored by thin-layer chromatography (TLC) carried out on 0.25 mm E. Merck silica gel plates (60F-254 or RP-18 F_{254s}) using UV light as the visualizing agent and an acidic solution of *p*-anisaldehyde, phosphomolybdic acid, cerric ammonium molybdate, Seebach's stain (PMA and CAM), ninhydrin, or potassium permanganate and heat as developing agents. E. Merck silica gel (60, particle size 0.043−0.063 mm) was used for flash column chromatography.

General Procedure for Oxidation using TFDO Generated in situ. The substrate (0.2 mmol) was dissolved in MeCN (6.0 mL, 0.03 M) by stirring and sonicating. To this solution was added aqueous sodium phosphate buffer (6.0 mL, pH = 7.5, 25 mM) and aqueous Na_2EDTA (1.3 mL, 40 mM). The solution was then cooled to 4 °C (ambient temperature), and cool (4 °C) 1,1,1-trifluoroacetone (0.143 mL, 1.60 mmol, 8.0 equiv) was added. Oxone ($KHSO_5$·0.5$KHSO_4$·0.5K_2SO_4, 738 mg, 2.4 mmol, 12 equiv) was then added in a single portion, and the suspension was rapidly stirred for 36 h. Then, the mixture was warmed to room temperature and extracted with Et_2O (3 × 15 mL). The combined organic layers were washed with brine (50 mL), dried over $MgSO_4$, filtered, and concentrated.

dx.doi.org/10.1021/jo400350v | J. Org. Chem. 2013, 78, 4037−4048

Similar conditions for in situ dioxirane formation for C−H oxidation have been developed.[51] References 21, 52, and 53 include spectral data for the sclareolide oxidation products. Reference 54 includes data for the products from oxidation of 1,3-dimethylcyclohexanes. *tert*-Butyl trifluoromethyl ketone could be synthesized according to ref 55. Alternatively, CF_3TMS could be added dropwise to a mixture of methyl pivalate and excess CsF at 0 °C.

■ ASSOCIATED CONTENT

Supporting Information

Tables and figures giving optimized Cartesian coordinates of all stationary points and saddle points and text giving the full ref 32. This material is available free of charge via the Internet at http://pubs.acs.org.

■ AUTHOR INFORMATION

Corresponding Author

*E-mail: houk@chem.ucla.edu (K.N.H.); robert.paton@chem.ox.ac.uk (R.S.P.).

Notes

The authors declare no competing financial interest.

■ ACKNOWLEDGMENTS

We are grateful to the Royal Commission for the Exhibition of 1851 for a Research Fellowship (R.S.P.), the National Institute of General Medical Sciences, National Institutes of Health (GM36700 to K.N.H. and GM097444 to P.S.B.), the TEVA Pharmaceuticals Scholars Grant (to P.S.B.), and Bristol-Myers Squibb (graduate fellowship to T.R.N.). Computations were performed using the UCLA Academic Technology Services Hoffman2 Beowulf cluster and the San Diego Supercomputer Center Thresher cluster. We thank Professor Yu Lan, Chongqing University, for helpful discussions.

■ REFERENCES

(1) Yamaguchi, J.; Yamaguchi, A. D.; Itami, K. *Angew. Chem., Int. Ed.* **2012**, *51*, 8960.
(2) Doyle, M. P.; Goldberg, K. I. *Acc. Chem. Res.* **2012**, *45*, 777.
(3) Crabtree, R. H. *Chem. Rev.* **2010**, *110*, 575.
(4) Brueckl, T.; Baxter, R. D.; Ishihara, Y.; Baran, P. S. *Acc. Chem. Res.* **2012**, *45*, 826.
(5) For recent reviews, see: (a) Davies, H. M. L.; Beckwith, R. E. J. *Chem. Rev.* **2003**, *103*, 2861. (b) Punniyamurthy, T.; Velusamy, S.; Iqbal, J. *Chem. Rev.* **2005**, *105*, 2329. (c) Godula, K.; Sames, D. *Science* **2006**, *312*, 67. (d) Dick, A. R.; Sanford, M. S. *Tetrahedron* **2006**, *62*, 2439. (e) Davies, H. M. L.; Manning, J. R. *Nature* **2008**, *451*, 417. (f) Giri, R.; Shi, B.-F.; Engle, K. M.; Maugel, N.; Yu, J.-Q. *Chem. Soc. Rev.* **2009**, *38*, 3242. (g) Daugulis, O.; Do, H.-Q.; Shabashov, D. *Acc. Chem. Res.* **2009**, *42*, 1074. (h) Mkhalid, I. A. I.; Barnard, J. H.; Marder, T. B.; Murphy, J. M.; Hartwig, J. F. *Chem. Rev.* **2010**, *110*, 890. (i) Shul'pin, G. B. *Org. Biomol. Chem.* **2010**, *8*, 4217. (j) Jazzar, R.; Hitce, J.; Renaudat, A.; Sofack-Kreutzer, J.; Baudoin, O. *Chem. Eur. J.* **2010**, *16*, 2654. (k) Lyons, T. W.; Sanford, M. S. *Chem. Rev.* **2010**, *110*, 1147. (l) C-H Activation. In *Topics in Current Chemistry*; Yu, J.-Q., Shi, Z., Eds.; Springer: Berlin, 2010; p 292. (m) Doyle, M. P.; Duffy, R.; Ratnikov, M.; Zhou, L. *Chem. Rev.* **2010**, *110*, 704. (n) Roizen, J. L.; Harvey, M. E.; Du Bois, J. *Acc. Chem. Res.* **2012**, *45*, 911.
(6) Murray, R. W.; Jeyaraman, R. *J. Org. Chem.* **1985**, *50*, 2847.
(7) Mello, R.; Fiorentino, M.; Sciacovelli, O.; Curci, R. *J. Org. Chem.* **1988**, *53*, 3890.
(8) Curci, R.; D'Accolti, L.; Fusco, C. *Acc. Chem. Res.* **2006**, *39*, 1.
(9) Curci, R.; Dinoi, A.; Rubino, M. F. *Pure Appl. Chem.* **1995**, *67*, 811.
(10) Bravo, A.; Bjorsvik, H. R.; Fontana, F.; Minisci, F.; Serri, A. *J. Org. Chem.* **1996**, *61*, 9409.
(11) Curci, R.; Dinoi, A.; Fusco, C.; Lillo, M. A. *Tetrahedron Lett.* **1996**, *37*, 249.
(12) Bravo, A.; Fontana, F.; Fronza, G.; Minisci, F.; Zhao, L. H. *J. Org. Chem.* **1998**, *63*, 254.
(13) Romney, D. K.; Miller, S. J. *Org. Lett.* **2012**, *14*, 1138.
(14) Newhouse, T.; Baran, P. S. *Angew. Chem., Int. Ed.* **2011**, *50*, 3362.
(15) Barton, D. H. R. *J. Chem. Soc.* **1953**, 1027.
(16) Barton, D. H. R.; Beviere, S. D.; Chavasiri, W.; Csuhai, E.; Doller, D.; Liu, W. G. *J. Am. Chem. Soc.* **1992**, *114*, 2147.
(17) Schreiber, J.; Eschenmoser, A. *Helv. Chim. Acta* **1955**, *38*, 1529.
(18) D'Accolti, L.; Fiorentino, M.; Fusco, C.; Rosa, A. M.; Curci, R. *Tetrahedron Lett.* **1999**, *40*, 8023.
(19) Mello, R.; Fiorentino, M.; Fusco, C.; Curci, R. *J. Am. Chem. Soc.* **1989**, *111*, 6749.
(20) (a) Gonzalez-Nunez, M. E.; Castellano, G.; Andreu, C.; Royo, J.; Baguena, M.; Mello, R.; Asensio, G. *J. Am. Chem. Soc.* **2001**, *123*, 7487. (b) Gonzalez-Nunez, M. E.; Royo, J.; Mello, R.; Baguena, M.; Ferrer, J. M.; de Arellano, C. R.; Asensio, G.; Prakash, G. K. S. *J. Org. Chem.* **2005**, *70*, 7919.
(21) Chen, M. S.; White, M. C. *Science* **2010**, *327*, 566.
(22) Chen, M. S.; White, M. C. *Science* **2007**, *318*, 783.
(23) Ishihara, Y.; Baran, P. S. *Synlett* **2010**, 1733.
(24) Chen, K.; Baran, P. S. *Nature* **2009**, *459*, 824.
(25) Chen, K.; Eschenmoser, A.; Baran, P. S. *Angew. Chem., Int. Ed.* **2009**, *48*, 9705.
(26) Du, X. H.; Houk, K. N. *J. Org. Chem.* **1998**, *63*, 6480.
(27) Glukhovtsev, M. N.; Canepa, C.; Bach, R. D. *J. Am. Chem. Soc.* **1998**, *120*, 10528.
(28) Paton, R. S.; Kim, S.; Ross, A. G.; Danishefsky, S. J.; Houk, K. N. *Angew. Chem., Int. Ed.* **2011**, *50*, 10366.
(29) Lan, Y.; Houk, K. N. *J. Am. Chem. Soc.* **2010**, *132*, 17921.
(30) Ess, D. H.; Houk, K. N. *J. Am. Chem. Soc.* **2008**, *130*, 10187.
(31) Ess, D. H.; Houk, K. N. *J. Am. Chem. Soc.* **2007**, *129*, 10646.
(32) Frisch, et al. *Gaussian 09, B.01 ed.*; Gaussian, Inc., Wallingford, CT, 2009.
(33) Aquilante, F.; De Vico, L.; Ferre, N.; Ghigo, G.; Malmqvist, P. A.; Neogrady, P.; Pedersen, T. B.; Pitonak, M.; Reiher, M.; Roos, B. O.; Serrano-Andres, L.; Urban, M.; Veryazov, V.; Lindh, R. *J. Comput. Chem.* **2010**, *31*, 224.
(34) Harding, L. B.; Goddard, W. A. *J. Am. Chem. Soc.* **1978**, *100*, 7180.
(35) Wadt, W. R.; Goddard, W. A. *J. Am. Chem. Soc.* **1975**, *97*, 3004.
(36) Bach, R. D.; Andres, J. L.; Owensby, A. L.; Schlegel, H. B.; Mcdouall, J. J. W. *J. Am. Chem. Soc.* **1992**, *114*, 7207.
(37) Shustov, G. V.; Rauk, A. *J. Org. Chem.* **1998**, *63*, 5413.
(38) Freccero, M.; Gandolfi, R.; Sarzi-Amade, M.; Rastelli, A. *Tetrahedron Lett.* **2001**, *42*, 2739.
(39) Freccero, M.; Gandolfi, R.; Sarzi-Amade, M.; Rastelli, A. *J. Org. Chem.* **2003**, *68*, 811.
(40) Fokin, A. A.; Tkachenko, B. A.; Korshunov, O. I.; Gunchenko, P. A.; Schreiner, P. R. *J. Am. Chem. Soc.* **2001**, *123*, 11248.
(41) Cremer, D.; Kraka, E.; Szalay, P. G. *Chem. Phys. Lett.* **1998**, *292*, 97.
(42) Ensing, B.; Buda, F.; Gribnau, M. C. M.; Baerends, E. J. *J. Am. Chem. Soc.* **2004**, *126*, 4355.
(43) Kumar, D.; de Visser, S. P.; Shaik, S. *J. Am. Chem. Soc.* **2003**, *125*, 13024.
(44) Wu, Y. D.; Houk, K. N. *J. Am. Chem. Soc.* **1987**, *109*, 908.
(45) Wu, Y. D.; Houk, K. N.; Trost, B. M. *J. Am. Chem. Soc.* **1987**, *109*, 5560.
(46) Damm, W.; Giese, B.; Hartung, J.; Hasskerl, T.; Houk, K. N.; Zipse, H. *J. Am. Chem. Soc.* **1992**, *114*, 4067.
(47) Luo, Y. R. *CRC Handbook of Chemistry and Physics*, 91st ed; CRC Press: Boca Raton, FL, 2010.
(48) Gordon, C. G.; Mackey, J. L.; Jewett, J. C.; Sletten, E. M.; Houk, K. N.; Bertozzi, C. R. *J. Am. Chem. Soc.* **2012**, *134*, 9199.
(49) Newhouse, T. Ph.D. thesis (with P. S. Baran); see the Supporting Information for details.

(50) (a) Liu, W.; Groves, J. T. *J. Am. Chem. Soc.* **2010**, *132*, 12847. (b) Liu, W.; Huang, X.; Cheng, M.-J.; Nielsen, R. J.; Goddard, W. A., III; Groves, J. T. *Science* **2012**, *337*, 1322.
(51) Annese, C.; D'Accolti, L.; Fusco, C.; Curci, R. *Org. Lett.* **2011**, *13*, 2142.
(52) Cambie, R. C.; Joblin, K. N.; McCallum, N. K. *Aust. J. Chem.* **1970**, *23*, 1439.
(53) Choudhary, M. I.; Musharraf, S. G.; Sami, A.; Rahman, A.-u. *Helv. Chim. Acta* **2004**, *87*, 2685.
(54) Senda, Y.; Ishiyama, J.; Imaizumi, S. *Tetrahedron* **1975**, *31*, 1601.
(55) Wiedemann, J.; Heiner, T.; Mloston, G.; Prakash, G. K. S.; Olah, G. H. *Angew. Chem., Int. Ed.* **1998**, *37*, 820.